

Article

Theoretical Study on the Thermal Degradation Process of Nylon 6 and Polyhydroxybutyrate

Yuliia Didovets  and Mateusz Z. Brela * 

Faculty of Chemistry, Jagiellonian University, Gronostajowa 2, 30-387 Cracow, Poland

* Correspondence: brela@chemia.uj.edu.pl

Abstract: This work presents the study of the thermal degradation process of two selected polymers: nylon 6 and polyhydroxybutyrate (PHB), representatives of polyamides and polyesters, frequently used nowadays. It is extremely important to specify optimal conditions that would allow a non-toxic and fast reprocessing of polymers in the plastic industry. The Density Functional Theory (DFT) method and a set of various computational details were applied to investigate the influence of the solvent presence and the rise of temperature on the thermodynamics of the degradation process. Obtained results were compared for both of the studied polymers, highlighting observed similarities. External conditions leading to the spontaneity of the nylon 6 thermal degradation process have been estimated. The results described in this paper can be useful in future research works investigating biodegradation conditions of the studied polymers.

Keywords: DFT; nylon 6; PHB; degradation process



Citation: Didovets, Y.; Brela, M.Z. Theoretical Study on the Thermal Degradation Process of Nylon 6 and Polyhydroxybutyrate. *Physchem* **2022**, *2*, 334–346. <https://doi.org/10.3390/physchem2040024>

Academic Editor: Vincenzo Barone

Received: 4 August 2022

Accepted: 6 October 2022

Published: 17 October 2022

Publisher's Note: MDPI stays neutral with regard to jurisdictional claims in published maps and institutional affiliations.



Copyright: © 2022 by the authors. Licensee MDPI, Basel, Switzerland. This article is an open access article distributed under the terms and conditions of the Creative Commons Attribution (CC BY) license (<https://creativecommons.org/licenses/by/4.0/>).

1. Introduction

Polymer materials have become irreplaceable in modern life. Synthetic and natural polymers are efficient in various applications, from medical tools to food packaging. However, polymer processing can lead to the formation of toxic volatile products of the thermal degradation process. For this reason, the detailed mechanism investigation, as well as the optimal conditions description of the process is essential.

In this research, we investigate and compare two types of polymers: polyamides and polyesters. Polyamides are a group of synthetic polymers widely used in various fields due to their beneficial properties. Depending on the synthesis process and the final molecular weight, polyamides, often named nylons, exhibit chemical and thermal resistance, elasticity and stiffness. One of the most manufactured nylons is nylon 6, generally formed from caprolactam as a result of ring-opening polymerization [1]. Nylon 6 consists of a six-carbon chain with amide and carbonyl functional groups; the chemical structure of nylon 6 is depicted in Figure 1. The polymer possesses properties typical for all nylons, that is why it is frequently used in the textile, plastic, electronic and food industries [1,2].

Nylon 6 commonly occurs in the two most stable crystal forms: the α form is reported to be thermodynamically favored, while the γ form is kinetically favored. Both nylon 6 polymorphs form strong interchain hydrogen bonds, which are partially responsible for specific polymer properties [3]. Nylon 6 crystal structure was investigated by means of experimental [4–6] and theoretical [3–9] methods.

Polyesters, in contrast to polyamides, include polymers that may naturally occur—an important example is polyhydroxyalkanoates (PHAs). Some microorganisms are known to synthesize PHAs under nutrient-limited conditions. Biocompatibility, nontoxicity and thermoplasticity are valuable qualities of PHAs [10]. One of the most studied members of the polyhydroxyalkanoate polymer family is polyhydroxybutyrate (PHB)—a four-carbon linear polymer, which comprises carbonyl and hydroxyl functional groups (Figure 1). PHB is mainly applied in medicine as the biocompatible and biodegradable component of

implants, artificial tissues and surgical sutures [10], as well as in the food industry as a packaging material [11].

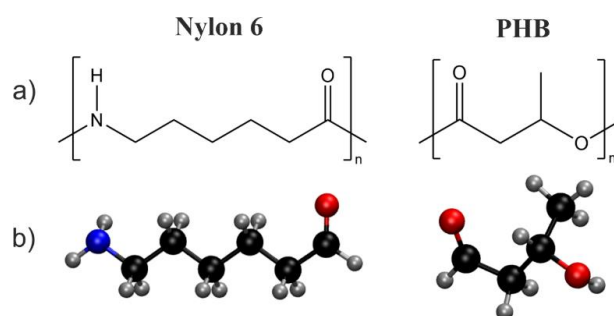


Figure 1. Structure of nylon 6 and polyhydroxybutyrate polymers: (a) structural formula of the polymer, (b) chemical structure of polymer monomer; the colors of the spheres are as follows: black—carbon, light grey—hydrogen, red—oxygen, blue—nitrogen.

Polyhydroxybutyrate crystallizes in two possible forms: the α helical form containing strong intermolecular interactions and the β planar-zigzag form [12]. Crystal structure and physical properties of PHB were studied both experimentally [12–15] and theoretically [12,14,16].

Polymer degradation is typically defined as a complex multi-staged process of polymer structural transformations, resulting in the formation of smaller fragments. The initial part of this process is interchain bonds' breaking, which contributes to the release of separate polymer chains. Major structural modifications happen during the last step of the degradation process—single polymer chain degradation. This is the key step of the process as a whole, consequently, it is the one that is investigated regularly. Under high-temperature conditions, a polymer can undergo thermal degradation due to strengthened intramolecular vibrations, which, in turn, are capable of breaking intrachain bonds [17].

Thermal degradation of nylon 6 polymer is frequently studied by thermogravimetry, differential scanning calorimetry, pyrolysis-gas-chromatography and infrared spectroscopy [18–20]. Previous research by Holland et al. [18] and Lehrle et al. [19] highlighted the two most probable mechanisms of the process: “crosslinking” and “end-biting”. The final product of both mechanisms is caprolactam and further polymer chain, however, the difference lies in structural transformations taking place in the early steps of the process. During the “end-biting” mechanism, the polymer chain bends from the terminal side, during the “crosslinking” mechanism, the inner mers of the polymer undergo bending. In this research, we assumed the “end-biting” mechanism of the nylon 6 thermal degradation process. Model structures of nylon 6 in different stages of the process—the substrate (N1), intermediate structure (N2) and the final product (N3)—are depicted in Figure 2.

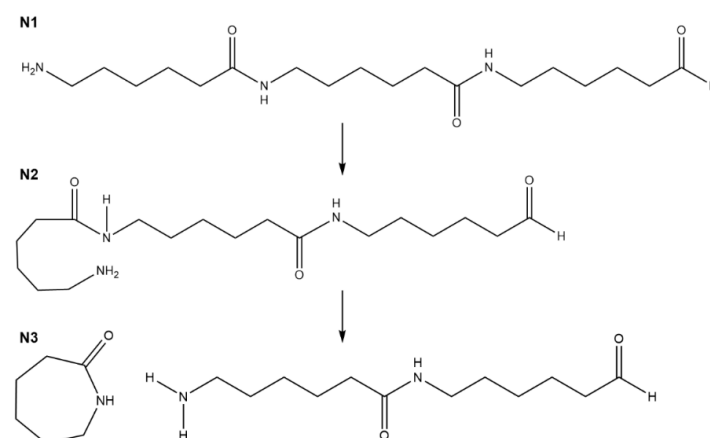


Figure 2. Mechanism of the thermal degradation of nylon 6: substrate (N1), intermediate structure (N2) and the final product (N3).

Polyhydroxybutyrate undergoes thermal degradation at a temperature near 180 °C, yielding oligomers of the polymer and crotonic acid in the random chain scission reaction [11,21]. Nevertheless, we suppose that the degradation mechanism, analogous to assumed for nylon 6, can also occur, but with the participation of two terminal mers, due to the critically small size of the PHB mer. We provide model structures of the substrate (P1), intermediate structures (P2, P3) and the final product (P4) of the PHB thermal degradation process in Figure 3.

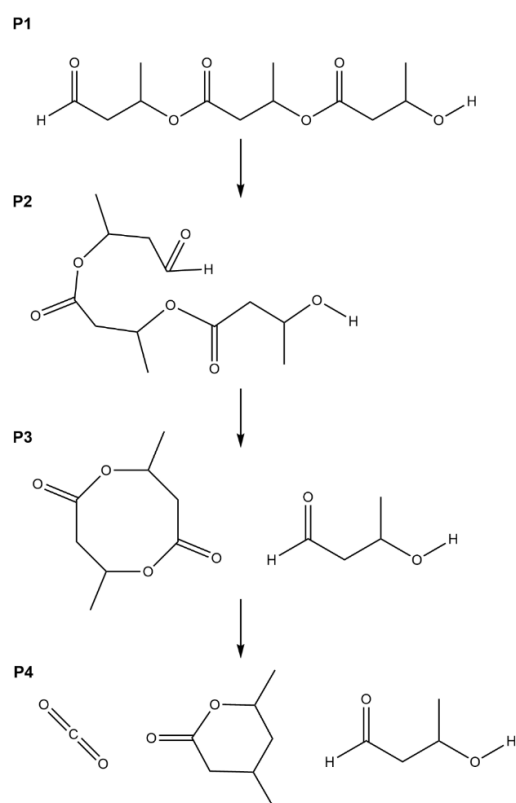


Figure 3. Mechanism of the thermal degradation of polyhydroxybutyrate (PHB): substrate (P1), intermediate structures (P2, P3) and the final product (P4).

Theoretical methods are known for accurate prediction of the system's properties and are successfully used as reliable support for experimental investigations. In spite of that, these methods are rarely chosen as tools for polymer degradation investigation. Our work represents an attempt to obtain trustworthy information about the studied process. The aim of our research is to provide a detailed description of the solvent presence and rise in temperature effect on the thermodynamic profile of nylon 6 and PHB thermal degradation processes by applying quantum-chemical calculations.

2. Materials and Methods

As was mentioned above, the thermal degradation of the single polymer chain is crucial in the thermal degradation of the polymer as a whole. Therefore, the trimer of the studied polymer has been applied as a computational model. Figures 4 and 5 depict the substrate, intermediate structures and final products of thermal degradation processes for both of the studied polymers, nylon 6 and PHB, respectively. Shown structures were exactly the ones used in the research. It is important to note, that the final products for both polymers, as well as the second intermediate structure of the PHB model (P3), were considered adducts in all calculations. In this case, a basis set superposition error (BSSE) was eliminated.

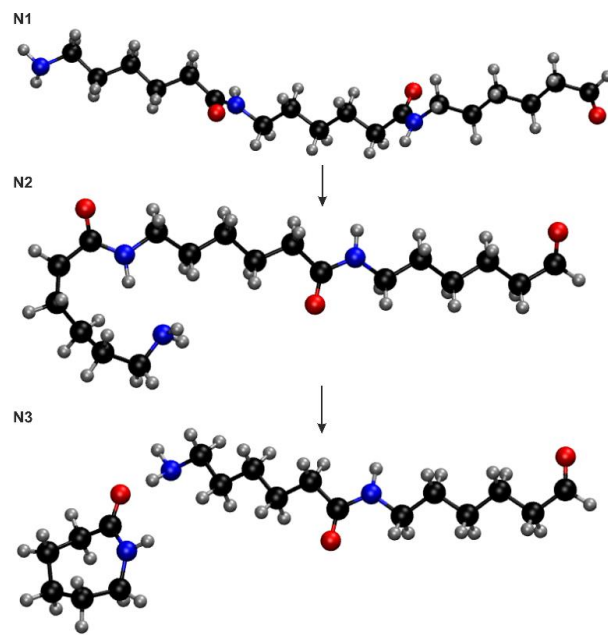


Figure 4. Chemical structure of the substrate (N1), intermediate structure (N2) and the final product (N3) of the nylon 6 thermal degradation process; the colors of the spheres are as follows: black—carbon, light grey—hydrogen, red—oxygen, blue—nitrogen.

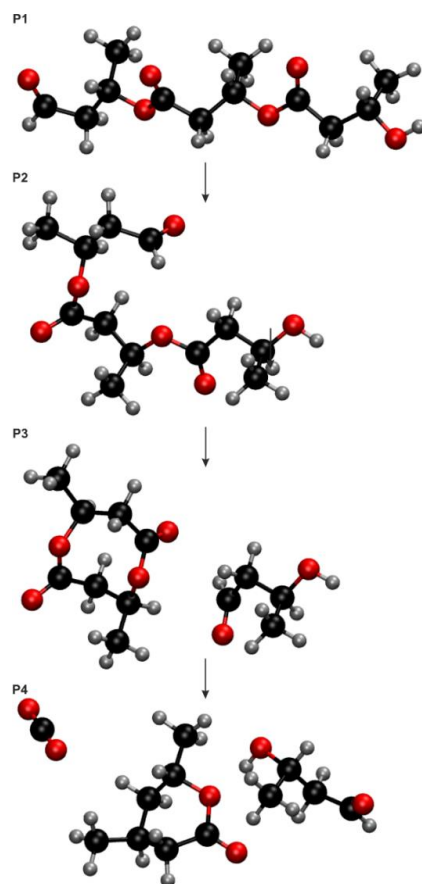


Figure 5. Chemical structure of the substrate (P1), intermediate structures (P2, P3) and the final product (P4) of the PHB thermal degradation process; the colors of the spheres are as follows: black—carbon, light grey—hydrogen, red—oxygen.

Quantum mechanical calculations were performed in ADF2019 [22–24] software. A DFT method with B3LYP [25,26] and BP86 [27,28] functionals was used, additionally taking into account Grimme's dispersion correction [29]. Three basis sets, TZP, TZ2P and QZ4P, were used. The solvation effect was investigated by means of the implicit COSMO [30] model, where water was considered a solvent. As far as electronic energy is independent of temperature, thermodynamic calculations were also performed, resulting in entropy, enthalpy and Gibbs free energies values. The temperature ranged from 298 K to 673 K. Stationary points were proved by vibrational analysis. All calculations were carried out on the Prometheus supercomputer from ACC Cyfronet AGH. The visualization of polymer structures was performed in VMD software [31], and the graphs were created in CorelDraw2020 software.

After performing the optimization calculations, computational models (trimers) of both polymers underwent partial bending, however intermediate structures, as well as final products, remained unchanged. Corresponding energies will be discussed in the "Computational details effect" section.

3. Results and Discussion

This research is divided into several parts. In the beginning, we investigated the effect of the computational details on obtained results. This was performed as a precaution against the so-called "basis set error" in particular, and to choose computational details optimal for researched compounds. Further, we have compared the results obtained in the "gas phase", meaning the model system without solvent, and in a presence of a solvent (solvation effect); as well as those for structures in different temperatures in the "gas phase" (temperature effect). Finally, we took into account both the presence of a solvent and the increasing temperature of the system to observe the complex effect of both external conditions on the thermodynamic profiles of nylon 6 and PHB thermal degradation processes. Enthalpy and entropy contributions to Gibbs free energy are briefly described in the last part.

3.1. Computational Details Effect

Electron energies of nylon 6 and PHB models (Figures 4 and 5) related to the substrate energy in both cases, N1 and P1, respectively, are presented in Figure 6. The top panel of Figure 6 represents the relative electron energies of nylon 6 structures, while the bottom panel represents the relative electron energies of PHB structures. Full data is available in Supplementary Materials, Tables S1 and S2.

For both of the polymers, including the dispersion correction (red and green lines in Figure 6) in calculations led to the decrease in relative electron energies of the intermediate structure and the final product of the thermal degradation process. However, for nylon 6 structures, the observed decrease in relative electron energies is more significant and causes the reversal of the thermodynamic profile of the process. We suppose that it directly corresponds to the highly polarized amide bond in the nylon 6 mers. Therefore, dispersion interactions, especially van der Waals interactions, cannot be neglected and make up a huge part of total electron energy. Polyhydroxybutyrate, on the contrary, contains ester bonds in the chemical structure of each mer, which is less polarized, so that included dispersion correction does not affect the total electron energy considerably. The difference in polarization of mentioned bonds can be clearly seen in the molecular electrostatic potential maps for both polymers, depicted in Figure 7.

The results obtained for different functionals (black and blue lines in Figure 6) are approximately consistent for different basis sets; for nylon 6 structures, a slight increase in relative electron energies is observed with the increase in the size of the basis set. Whereas for different functionals with dispersion correction the results' consistency with the size of the basis set is kept only for PHB structures, for nylon 6 structures only relative electron energies calculated by the use of BP86 functional remain nearly unchanged.

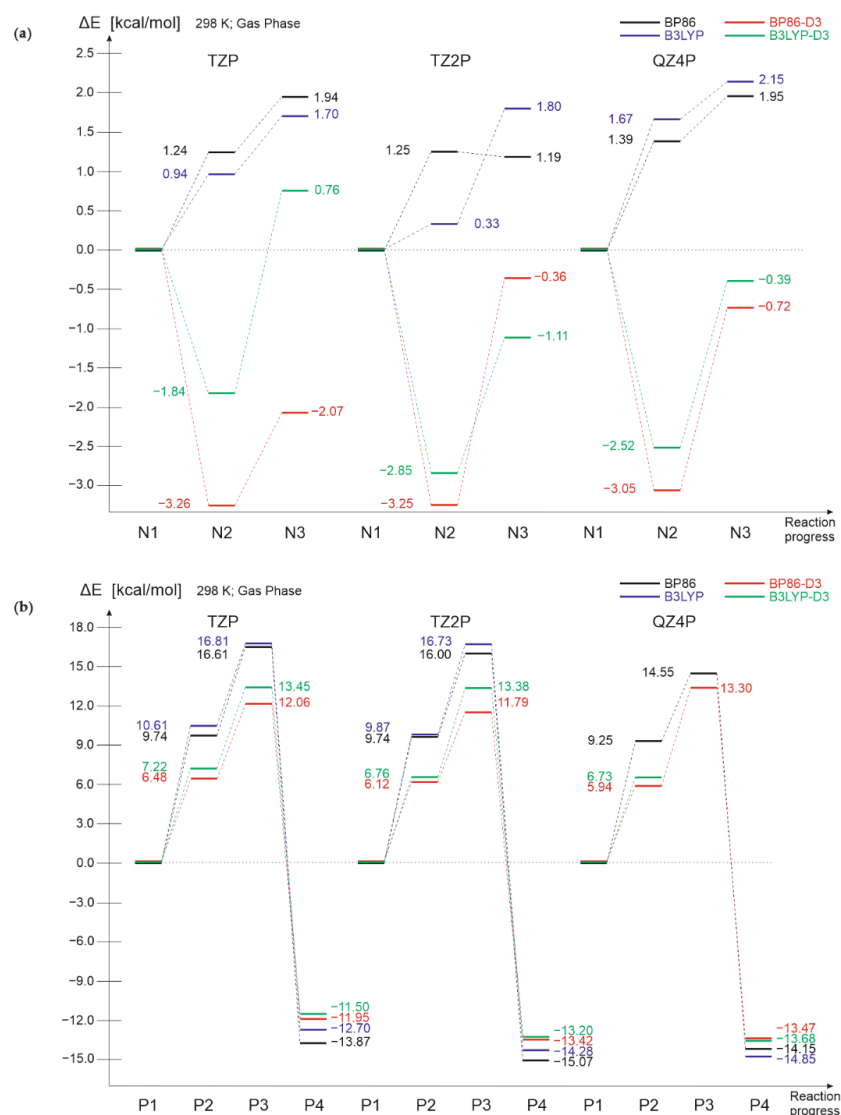


Figure 6. Relative electron energies of (a) nylon 6 and (b) PHB structures obtained using different computational details; labels of the structures correspond to given in Figure 2, Figure 3, Figure 4, Figure 5.

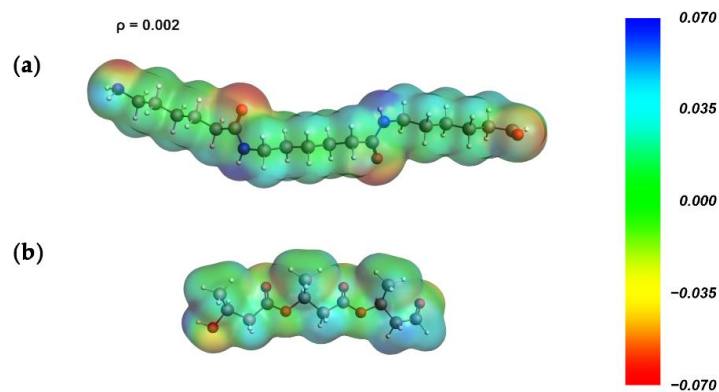


Figure 7. Molecular electrostatic potential map of (a) nylon 6 and (b) PHB models.

The analysis of the computational details effect allowed us to estimate, that the BP86-D3/TZP details can be considered optimal for investigated polymer structures, and thus were chosen for further research.

3.2. Solvation Effect

Investigation of the solvation effect provides information about energy components from interactions between the solvent and the dissolved chemical compound. Gibbs free energies of nylon 6 and PHB structures with and without a solvent, related to the substrate energy, are represented in Figure 8. The top panel of Figure 8 shows results for nylon 6 structures, while the bottom panel—for PHB structures. Full data for all considered computational details is available in Supplementary Materials, Tables S3 and S4.

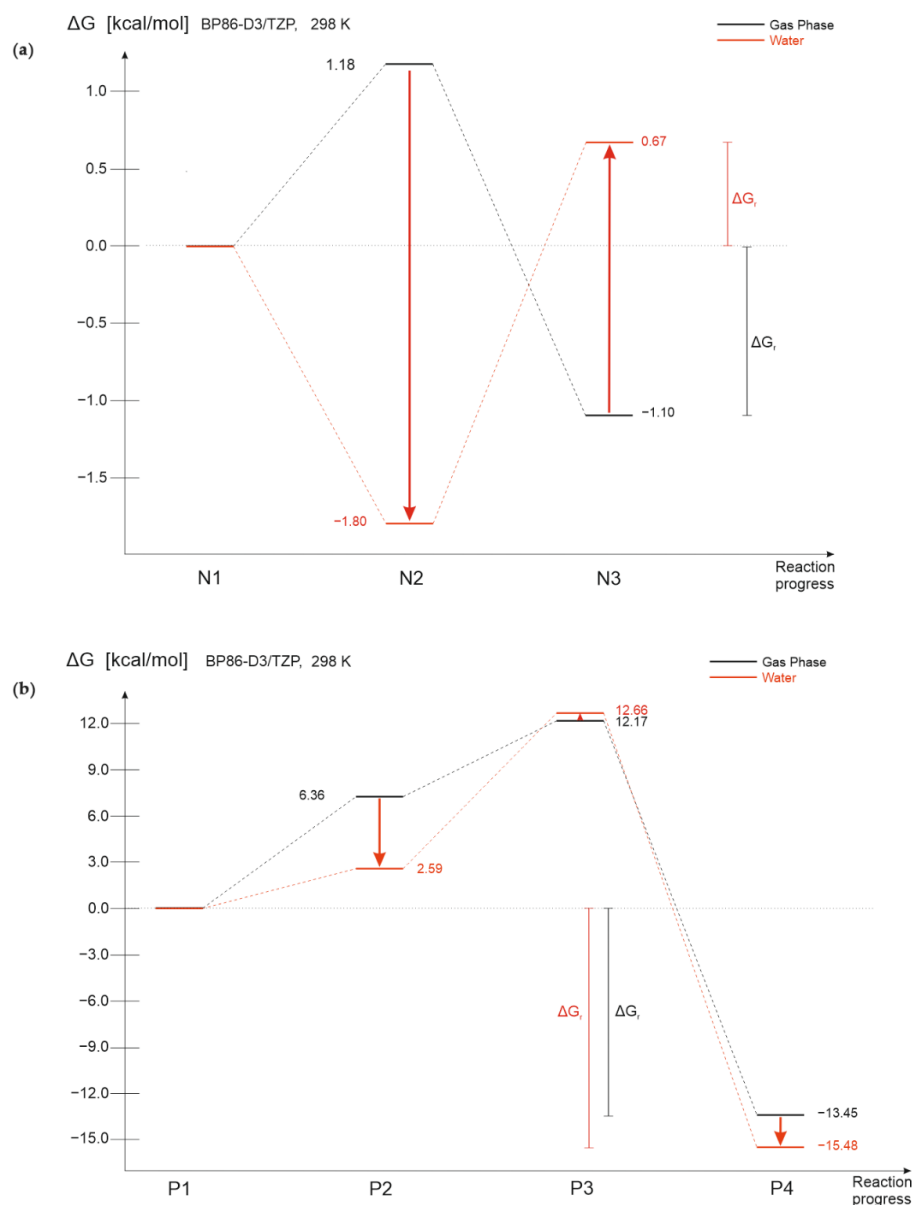


Figure 8. Relative Gibbs free energies of (a) nylon 6 and (b) PHB structures obtained for gas phase (black lines) and water presence (red lines) in 298 K.

The solvation effect on the thermodynamic profiles of thermal degradation processes turned out to be rather different. For the first intermediate structure, which is a bent polymer chain in both cases, the presence of a solvent leads to a decrease in relative Gibbs energies. This observation is most probably connected to forming of stabilizing interactions between polymer and water. However, the solvation effect on relative Gibbs energies of nylon 6 and PHB thermal degradation final products is opposite: while relative Gibbs energy of nylon 6 degradation final product significantly increases when adding

a solvent, relative Gibbs energy of PHB degradation final product decreases. In the first case, Gibbs free energy of the final product becomes higher than the substrate energy, thus estimating the last step of the degradation as non-spontaneous. The final product of the nylon 6 thermal degradation process is cyclic caprolactam and the dimer of the polymer. The solvent located between the caprolactam, and the dimer can interfere the electrostatic interactions between the amide group of the dimer and the carbonyl group of caprolactam, therefore causing an increase in the relative Gibbs free energy. The PHB degradation final product, oxygen atoms in its structure specifically, forms electrostatic interactions with water, decreasing the total relative Gibbs free energy of the product.

3.3. Temperature Effect

The effect of the increasing temperature on the thermodynamic profile of the thermal degradation process allows tracking total energy changes as a system's response to the temperature. For polymers, it is extremely important to cover the melting and degradation temperatures in the investigated range of temperatures. The temperature effect on the thermodynamic profile of nylon 6 and PHB thermal degradation process is represented in Figure 9 as changes in relative Gibbs free energies of model nylon 6 and PHB structures.

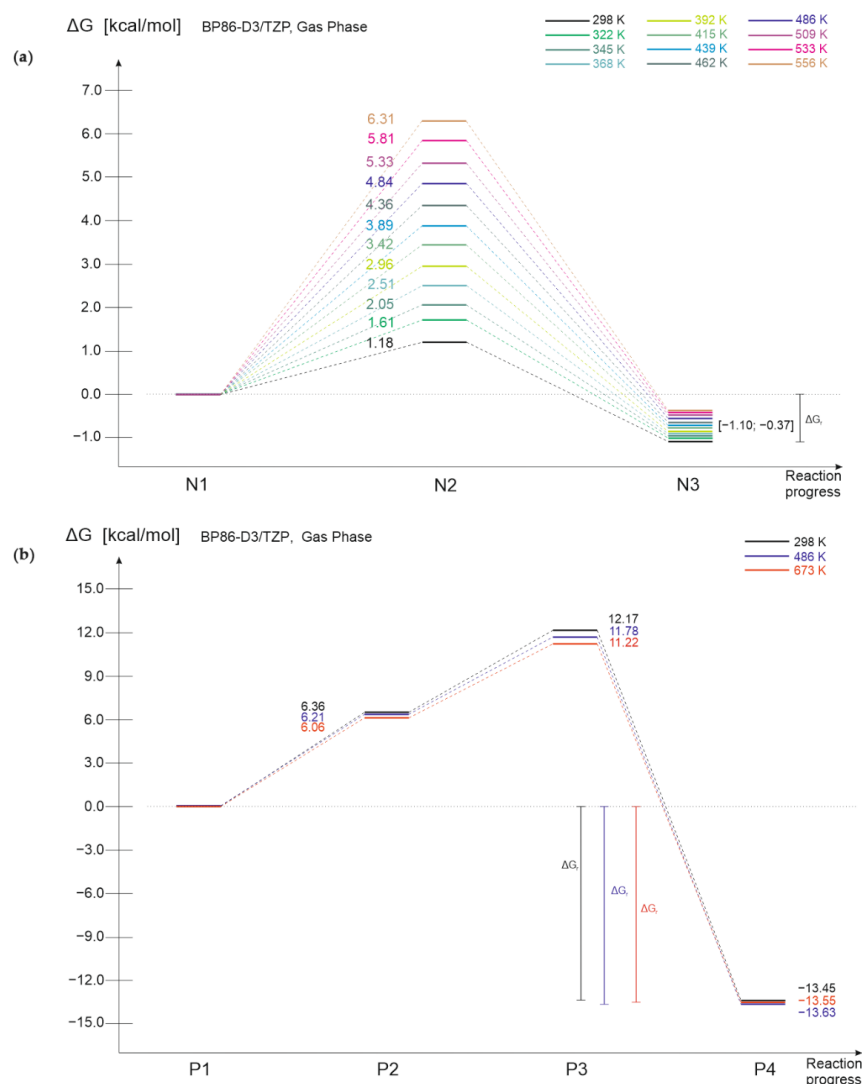


Figure 9. Relative Gibbs free energies of (a) nylon 6 and (b) PHB structures obtained in different temperatures in gas phase; some of the data was neglected aiming the clarity of the picture.

The rise of temperature leads to the increase of relative Gibbs free energies of intermediate structures for both polymers; however, the increase is more considerable in the case of nylon 6 (the top panel in Figure 9). Importantly, the growth of relative Gibbs free energy is proportional to the rise of temperature and does not change even after crossing the degradation temperature of the polymer (280 °C for nylon 6 [18], 180 °C for PHB [11]). Relative Gibbs free energies of final products remain nearly unchanged during the rise of temperature. Despite expectations, the rise of temperature singly does not lead to the spontaneity of the process.

3.4. Solvation and Temperature Effect

Investigation of solvent and temperature effects separately provides valuable information about the system’s response to these external conditions. Undoubtedly, considering both conditions simultaneously yields a more accurate description of thermodynamic effects. Figure 10 illustrates the relative Gibbs free energies of nylon 6 and PHB structures in selected temperatures with and without the presence of a solvent.

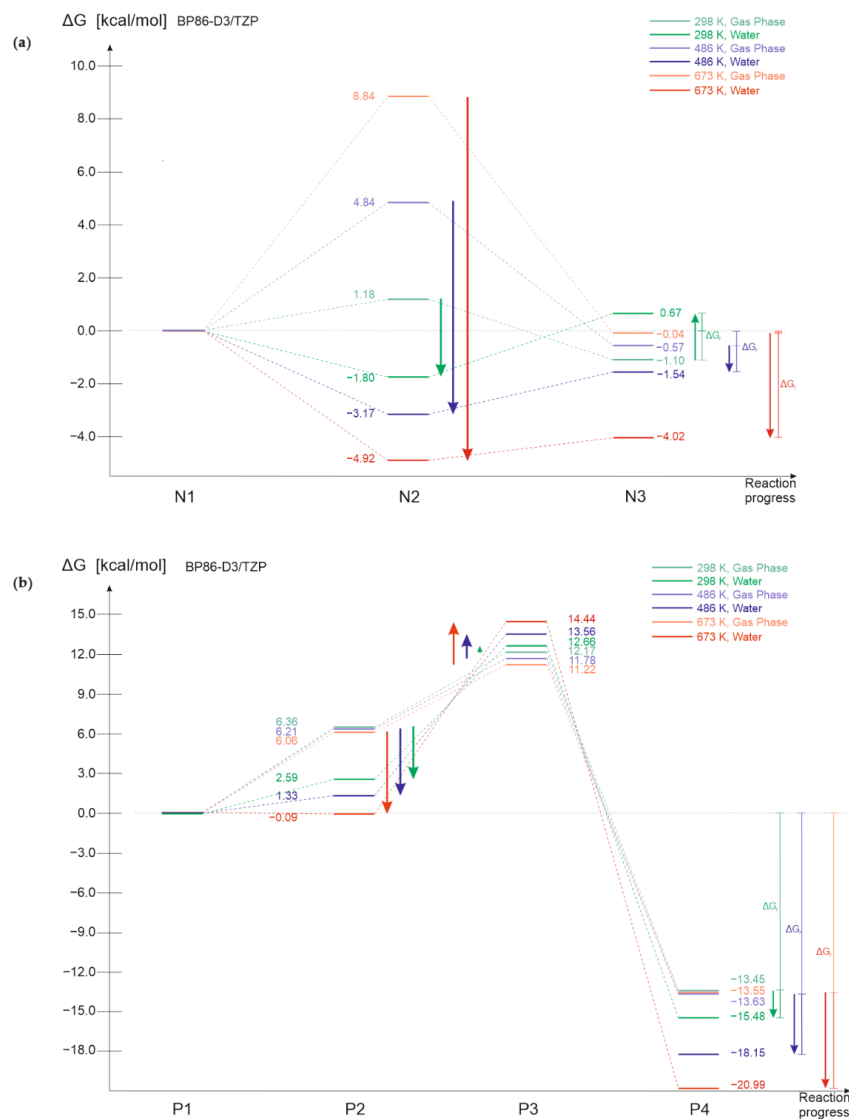


Figure 10. Relative Gibbs free energies of (a) nylon 6 and (b) PHB structures obtained for gas phase (low-saturation colors) and water presence (high-saturation colors) in different temperatures; some of the data was neglected aiming the clarity of the picture.

The rise of temperature with an addition of a solvent causes in general a decline in relative Gibbs free energies of nylon 6 and PHB structures. This observation leads to one of the main conclusions of our research—high temperature and the presence of a solvent can cause the spontaneity of the nylon 6 thermal degradation process. However, mentioned external conditions are not sufficient for spontaneity of the whole PHB thermal degradation process, only for the last step of the process.

3.5. Enthalpy and Entropy Contributions

When analyzing the data on the above graphs, it is important to remember, that enthalpy and entropy are two main constituents of free Gibbs energy, thus having a determinative impact on the final result. While the entropy and enthalpy terms are calculated on the basis of the partition function, Gibbs free energy, in turn, is obtained as follows [32]:

$$\Delta G = \Delta H - T\Delta S \quad (1)$$

The influence of entropy on thermodynamic profiles is decisive for nylon 6 and PHB, as it is reversing when the solvent presence is considered. On the other hand, the enthalpy contributions are not leading to significant changes in relative Gibbs energy. Relative enthalpies and entropies for both polymers are shown in Figure 11.

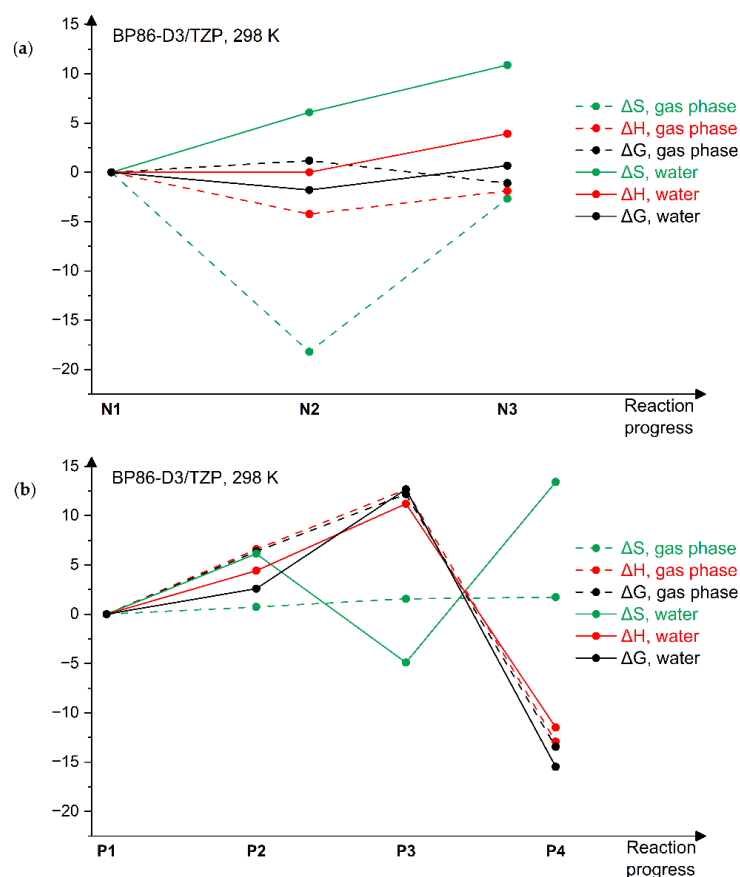


Figure 11. Enthalpy (red lines) and entropy (green lines) contributions to Gibbs free energies (black lines) of (a) nylon 6 and (b) PHB structures obtained for gas phase (dashed lines) and water presence (solid lines) in 298 K.

The relative entropy of nylon 6 increases when a solvent is added, therefore easing the reaction to proceed. The rise of relative enthalpy, on the contrary, determines the additional energy essential for the reaction's progress. Solvent presence affects the relative enthalpy and entropy of polyhydroxybutyrate differently. The increase in relative enthalpy is nearly

constant until the second intermediate structure (P3), afterwards it rapidly falls till the final product. Relative entropy changes clarify the reason for the possible spontaneity of the PHB thermal degradation last step.

Another important observation is the temperature dependence of enthalpy and entropy fluctuations and their general impact on the Gibbs free energy: the rise of temperature contributes to higher absolute values of relative enthalpy and entropy. Necessary graphs are provided in Supplementary Materials (Figures S1 and S2).

4. Conclusions

In this paper, we described the temperature and solvent presence impact on the thermodynamic profile of nylon 6 and PHB thermal degradation process by means of quantum-chemical calculations. The received results are summarized in Table 1. Despite the similarities in the thermal degradation mechanisms of nylon 6 and PHB, the solvent presence affects the thermodynamic profiles of the process oppositely. The rise of temperature and the simultaneous effect of both conditions, on the contrary, caused comparable changes in the thermodynamic profiles of the process for studied polymers. While analyzing the results we established, that the presence of a solvent has a greater impact on the thermodynamic profiles rather than the rise of temperature, due to the development of electrostatic interactions between the polymer and a solvent. Solvent presence is essential for the spontaneity of the nylon 6 degradation process, although high-temperature conditions should also be considered. Importantly, the dispersion correction included in the calculations proved to be relevant in the nylon 6 chemical structure investigation, but not crucial in the PHB chemical structure studies.

Table 1. Summary of investigated external conditions' effect on the thermodynamic profiles of nylon 6 and PHB thermal degradation processes.

	Nylon 6	PHB
Solvation effect	$\Delta G \downarrow$ intermediate structure $\Delta G \uparrow$ final product <i>reversed process profile</i>	$\Delta G \downarrow$ intermediate structure (P2) $\Delta G \uparrow$ intermediate structure (P3) $\Delta G \downarrow$ final product
Temperature effect	$\Delta G \uparrow$ intermediate structure $\Delta G \sim$ final product	$\Delta G \sim$ intermediate structures $\Delta G \sim$ final product
Solvation and temperature effect	$\Delta G \downarrow$ intermediate structure $\Delta G \downarrow$ final product <i>reversed process profile</i>	$\Delta G \downarrow$ intermediate structure (P2) $\Delta G \uparrow$ intermediate structure (P3) $\Delta G \downarrow$ final product

Undoubtedly, further research on the topic should include the application of a hybrid solvation model, considering both implicit solvent and explicitly added solvent molecules simultaneously. This approach will provide a more accurate description of short- and long-range interactions between the studied polymer and a solvent. Attention should also be put on other possible external conditions, especially the acidity of the environment, capable of starting the acid hydrolysis process.

Supplementary Materials: The following supporting information can be downloaded at: <https://www.mdpi.com/article/10.3390/physchem2040024/s1>, Table S1: Electron energies of nylon 6 structures related to the substrate (N1) electron energy in gas phase for different computational details, in kcal/mol.; Table S2: Electron energies of PHB structures related to the substrate (P1) electron energy in gas phase for different computational details, in kcal/mol.; Table S3: Gibbs free energies of nylon 6 structures related to the substrate (N1) Gibbs free energy in gas phase (298 K) for different computational details, in kcal/mol.; Table S4: Gibbs free energies of PHB structures related to the substrate (P1) Gibbs free energy in gas phase (298 K) for different computational details, in kcal/mol; Supplementary Material. Enthalpy (red lines) and entropy (green lines) contributions to Gibbs free energies (black lines) of (a) nylon 6 and (b) PHB structures obtained for gas phase (dashed lines) and water presence (solid lines) in 486 K; Figure S2. Enthalpy (red lines) and entropy (green lines) contributions to Gibbs free energies (black lines) of a) nylon 6 and b) PHB structures obtained for gas phase (dashed lines) and water presence (solid lines) in 673 K.

Author Contributions: Investigation, Y.D. and M.Z.B.; Conceptualization, Y.D. and M.Z.B.; Methodology, M.Z.B.; Data Analysis, Y.D.; Writing—Original Draft Preparation, Y.D.; Writing—Review and Editing, Y.D. and M.Z.B.; Supervision, M.Z.B. All authors have read and agreed to the published version of the manuscript.

Funding: This work was supported by grant IDUB/DigiWorld/2022/14 1027.0641.363.2019 from Jagiellonian University.

Data Availability Statement: The data supporting the findings of this study are available in the supplementary material of the article.

Acknowledgments: The results presented in this paper were obtained using PL-Grid Infrastructure and resources provided by ACC Cyfronet AGH. We thank the Priority Research Area DigiWorld under the program “Excellence Initiative –Research University” at the Jagiellonian University in Cracow for support.

Conflicts of Interest: The authors declare no conflict of interest.

References

1. Vagholkar, P. Nylon (Chemistry, Properties and Uses). *Int. J. Sci. Res.* **2016**, *5*, 349–351.
2. Sewidan, M. Nylon-6 (polyamide 6), Historical background, Properties and Limitations. Master’s Thesis, Mansoura University, Mansoura, Egypt, 2020.
3. Brela, M.Z.; Wójcik, M.J.; Boczar, M.; Onishi, E.; Sato, H.; Nakajima, T.; Ozaki, Y. Study of hydrogen bond dynamics in Nylon 6 crystals using IR spectroscopy and molecular dynamics focusing on the differences between α and γ crystal forms. *Int. J. Quantum Chem.* **2018**, *118*, e25595. [[CrossRef](#)]
4. Hoshina, H.; Kanemura, T.; Ruggiero, M.T. Exploring the Dynamics of Bound Water in Nylon Polymers with Terahertz Spectroscopy. *J. Phys. Chem. B* **2020**, *124*, 422–429. [[CrossRef](#)]
5. Yamamoto, S.; Ohnishi, E.; Sato, H.; Hoshina, H.; Ishikawa, D.; Ozaki, Y. Low-Frequency Vibrational Modes of Nylon 6 Studied by Using Infrared and Raman Spectroscopies and Density Functional Theory Calculations. *J. Phys. Chem. B* **2019**, *123*, 5368–5376. [[CrossRef](#)] [[PubMed](#)]
6. Morisawa, Y.; Yasunaga, M.; Sato, H.; Fukuda, R.; Ehara, M.; Ozaki, Y. Rydberg and π – π^* Transitions in Film Surfaces of Various Kinds of Nylons Studied by Attenuated Total Reflection Far-Ultraviolet Spectroscopy and Quantum Chemical Calculations: Peak Shifts in the Spectra and Their Relation to Nylon Structure and Hydrogen Bondings. *J. Phys. Chem. B* **2014**, *118*, 11855–11861. [[PubMed](#)]
7. Arabnejad, S.; Manzhos, S. Defects in alpha and gamma crystalline nylon6: A computational study. *AIP Adv.* **2015**, *5*, 107123. [[CrossRef](#)]
8. Quarti, C.; Milani, A.; Civalleri, B.; Orlando, R.; Castiglioni, C. Ab Initio Calculation of the Crystalline Structure and IR Spectrum of Polymers: Nylon 6 Polymorphs. *J. Phys. Chem. B* **2012**, *116*, 8299–8311. [[CrossRef](#)] [[PubMed](#)]
9. Milani, A. Unpolarized and Polarized Raman Spectroscopy of Nylon-6 Polymorphs: A Quantum Chemical Approach. *J. Phys. Chem. B* **2015**, *119*, 3868–3874. [[CrossRef](#)] [[PubMed](#)]
10. Kök, F.N.; Hasirci, V. Polyhydroxybutyrate and its copolymers: Applications in the medical field. In *Tissue Engineering and Novel Delivery Systems*; Taylor & Francis: Abingdon-on-Thames, UK, 2004; pp. 543–561.
11. Bugnicourt, E.; Cinelli, P.; Lazzeri, A.; Alvarez, V. Polyhydroxyalkanoate (PHA): Review of synthesis, characteristics, processing and potential applications in packaging. *Express Polym. Lett.* **2014**, *8*, 791–808. [[CrossRef](#)]
12. Wang, H.; Tashiro, K. Reinvestigation of Crystal Structure and Intermolecular Interactions of Biodegradable Poly(3-Hydroxybutyrate) α -Form and the Prediction of Its Mechanical Property. *Macromolecules* **2016**, *49*, 581–594. [[CrossRef](#)]
13. Pachekoski, W.M.; Dalmolin, C.; Agnelli, J.A.M. The Influence of the Industrial Processing on the Degradation of Poly(hydroxybutyrate)—PHB. *Mater. Res.* **2013**, *16*, 327–332. [[CrossRef](#)]
14. Beć, K.B.; Morisawa, Y.; Kobashi, K.; Grabska, J.; Tanabe, I.; Tanimura, E.; Sato, H.; Wójcik, M.J.; Ozaki, Y. Rydberg transitions as a probe for structural changes and phase transition at polymer surfaces: An ATR-FUV-DUV and quantum chemical study of poly(3-hydroxybutyrate) and its nanocomposite with graphene. *Phys. Chem. Chem. Phys.* **2018**, *20*, 8859. [[CrossRef](#)] [[PubMed](#)]
15. Phongtamrug, S.; Tashiro, K. X-ray Crystal Structure Analysis of Poly(3-hydroxybutyrate) β -Form and the Proposition of a Mechanism of the Stress-Induced α -to- β Phase Transition. *Macromolecules* **2019**, *52*, 2995–3009. [[CrossRef](#)]
16. Yamamoto, S.; Morisawa, Y.; Sato, H.; Hoshina, H.; Ozaki, Y. Quantum Mechanical Interpretation of Intermolecular Vibrational Modes of Crystalline Poly-(R)-3-Hydroxybutyrate Observed in Low-Frequency Raman and Terahertz Spectra. *J. Phys. Chem. B* **2013**, *117*, 2180–2187. [[CrossRef](#)]
17. Vohlidal, J. Polymer degradation: A short review. *CTI* **2021**, *3*, 213–220. [[CrossRef](#)]
18. Holland, B.J.; Hay, J.N. Thermal degradation of nylon polymers. *Polym. Int.* **2000**, *49*, 943–948. [[CrossRef](#)]
19. Lehrle, R.S.; Parsons, I.W.; Rollinson, M. Kinetics and Mechanisms of the Thermal Degradation of Nylon 6. In *Ageing Studies and Lifetime Extension of Materials*; Mallinson, L.G., Ed.; Springer: Boston, MA, USA, 2001; pp. 87–96.

20. Shahryar, P.; Siddaramaiah; Maziar, A.M.; Akheel, S.A. Thermal degradation kinetics of nylon6/GF/crysnano nanoclay nanocomposites by TGA. *Chem. Ind. Chem. Eng. Q.* **2011**, *17*, 141–151.
21. Kopinke, F.-D.; Remmler, M.; Mackenzie, K. Thermal decomposition of biodegradable polyesters—I: Poly(β -hydroxybutyric acid). *Polym. Degrad. Stab.* **1996**, *52*, 25–38. [[CrossRef](#)]
22. Velde, G.T.; Bickelhaupt, F.M.; Baerends, E.J.; Fonseca Guerra, C.; van Gisbergen, S.J.A.; Snijders, J.G.; Ziegler, T. Chemistry with ADF. *J. Comput. Chem.* **2001**, *22*, 931. [[CrossRef](#)]
23. Fonseca Guerra, C.; Snijders, J.G.; Velde, G.T.; Baerends, E.J. Towards an order-N DFT method. *Theor. Chem. Acc.* **1998**, *99*, 391. [[CrossRef](#)]
24. Baerends, E.J.; Ziegler, T.; Atkins, A.J.; Autschbach, J.; Baseggio, O.; Bashford, D.; Bérces, A.; Bickelhaupt, F.M.; Bo, C.; Boerrigter, P.M.; et al. *ADF2019, SCM, Theoretical Chemistry*; Vrije Universiteit: Amsterdam, The Netherlands. Available online: <http://www.scm.com> (accessed on 25 May 2019).
25. Becke, A.D. Density-functional thermochemistry. III. The role of exact exchange. *J. Chem. Phys.* **1993**, *98*, 5648–5652. [[CrossRef](#)]
26. Lee, C.; Yang, W.; Parr, R.G. Development of the Colle-Salvetti correlation-energy formula into a functional of the electron density. *Phys. Rev. B* **1988**, *37*, 785–789. [[CrossRef](#)]
27. Becke, A.D. Density-functional exchange-energy approximation with correct asymptotic-behavior. *Phys. Rev. A* **1988**, *38*, 3098–3100. [[CrossRef](#)]
28. Perdew, J.P. Density-functional approximation for the correlation energy of the inhomogeneous electron gas. *Phys. Rev. B* **1986**, *33*, 8822–8824. [[CrossRef](#)] [[PubMed](#)]
29. Grimme, S.; Antony, J.; Ehrlich, S.; Krieg, H. A consistent and accurate ab initio parameterization of density functional dispersion correction (DFT-D) for the 94 elements H-Pu. *J. Chem. Phys.* **2010**, *132*, 54104. [[CrossRef](#)] [[PubMed](#)]
30. Pye, C.C.; Ziegler, T. An implementation of the conductor-like screening model of solvation within the Amsterdam density functional package. *Theor. Chem. Acc.* **1999**, *101*, 396. [[CrossRef](#)]
31. Humphrey, W.; Dalke, A.; Schulten, K. VMD—Visual Molecular Dynamics. *J. Molec. Graphics* **1996**, *14*, 33–38. [[CrossRef](#)]
32. Jensen, F. *Introduction to Computational Chemistry*, 2nd ed.; John Wiley & Sons: Hoboken, NJ, USA, 2007; pp. 426–439.